PERGAMON

International Journal of Solids and Structures 38 (2001) 6889–6906

INTERNATIONAL JOURNAL OF SOLIDS and STRUCTURES

www.elsevier.com/locate/ijsolstr

A general solution on stress singularities in an anisotropic wedge

Ching-Hwei Chue *, Chuan-I Liu

Department of Mechanical Engineering, National Cheng Kung University, Tainan 70101, Taiwan, ROC

Received 21 March 2000; in revised form 18 January 2001

Abstract

This paper presents a general solution for determining the stress singularity order in an anisotropic wedge. The order depends on the wedge angle, boundary conditions and material properties. The characteristic equation, which governs the eigenvalues, is established from the Lekhnitskii's complex function method. A domain of one-quarter circle is proposed in which the contours of singularity order are plotted for all fiber orientations and a certain wedge angle. The numerical results agree well with the open literature for special cases. To reduce to strength of stress singularity at the wedge corner, the fiber direction corresponding to minimum singularity order can be determined.

Keywords: Stress singularity; Anisotropic wedge; Fiber orientation; Lekhnitskii's formulation

1. Introduction

In an elastic solid with geometric and/or material discontinuities, the stress may be singular. The nature of stress singularities for several wedge configurations has been studied in the past. By making use of the Mellin transform, Tranter (1948) obtained a formal solution for the stress distribution in an infinite wedge under fairly general conditions of surface loading. Williams (1952) used the Airy stress function and separation of variable to study the single-material wedge under different boundary conditions. He found that the stresses near the apex of an isotropic elastic wedge are proportional to $r^{\lambda-1}$ $(0 < \mathrm{Re}[\lambda] < 1)$. The value of $\lambda - 1$ can be real or complex in general. The severity of strong singularity order may cause cracks initiation and propagation at the apex of the wedge. Bogy (1971) employed the Mellin transform to treat the two-material wedge problem that are bonded together along a common wedge and subjected to surface traction at the boundaries. Dempsey and Sinclair (1979) utilized the separation of variables on the Airy stress function to derive conditions for stress singularities of the form $(r^{\lambda-1}\ln r)$ as $r \approx 0$. Many other researchers have studied related or extended wedge problems (see Erdogan, 1965; Hein and Erdogan, 1971; Theocaris, 1974; Chen and Nisitani, 1992, 1993; Koguchi et al., 1993; for example).

* Corresponding author. Tel.: +886-6-2757575, ext. 62165; fax: +886-6-2352973.
E-mail address: chchue@mail.ncku.edu.tw (C.-H. Chue).

0020-7683/01/$ - see front matter
PII: S0020-7683(01)00015-4

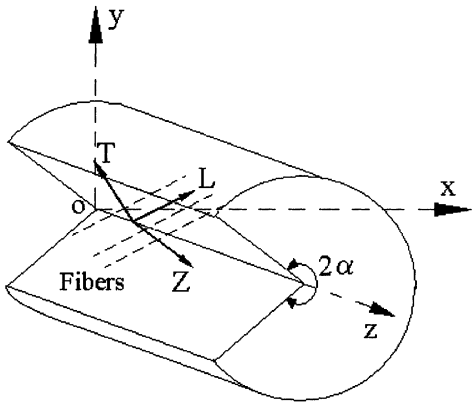

Fig. 1. Geometry of a wedge structure.

All of the above-mentioned research works are applied to isotropic elastic materials. Since composite materials have become widely used in engineering structure design, people now pay more attention to the anisotropic wedge problems. Fiber reinforced composites are commonly considered and modeled as orthotropic materials. Investigation of the associated crack problems for anisotropic materials was started by Sih et al. (1965).

When the composite reinforcing fibers lie in the x–y plane, the plane of elastic symmetry is normal to the z-axis (Fig. 1). The inplane and antiplane stress fields of generalized plane deformation problem are decoupled. Bogy (1972) and Kuo and Bogy (1974a,b) employed a complex function representation of the solution (Green and Zerna, 1954) in conjunction with a Mellin transform to analyze the inplane stress singularities in anisotropic wedges. Ma and Hour (1989) used Mellin transform to study the same wedge problem for antiplane stress singularities.

If the fibers of each layer lie in the y–z plane (e.g. Delale, 1984) or x–z plane (Lin and Hartmann, 1989), the material becomes fully anisotropic in global coordinates. The inplane and antiplane stress fields are coupled. The stress singularities for several special configurations of anisotropic materials have been discussed, such as at a free edge in laminated composites (Ting and Chou, 1981; Huang and Chen, 1994), bonded anisotropic wedges (Delale, 1984; Lin and Hartmann, 1989), and anisotropic layered composites with a crack normal to an interface (Ting and Hoang, 1984). Chen (1998) utilized Ting's formulation (Ting, 1986) to study the stress singularities in anisotropic multi-material wedges and junctions. Pageau and Biggers (1996) developed a finite element approach to analyze three-dimensional singular stress in prismatic configurations of anisotropic multi-material wedges and junctions. Wang and Choi (1982) employed Lekhnitskii's formulation to obtain the solution for a free edge laminates under extension. Based on the Stroh formulation (Stroh, 1962), Zwiers et al. (1982) found out the possible existence of logarithmic particular solutions for stress in free edge problems under uniform extension.

Based on the Lekhnitskii's formulations, this paper presents a general homogeneous solution to determine the singularity orders at the anisotropic wedge corner for any fiber orientation. One-quarter circular region with fiber orientation (ξ, η) as the coordinates is used to plot the variation of all singularity orders as contour lines in this region. The dependence of fiber orientation is easily seen from these plots and the fiber orientations to minimize the severity of the singularity can be determined visually.

The presence of the $r^{\lambda-1}$ type singularity in an eigenfunction does not assure us the existence of that particular singularity. It does tell us that, if a stress singularity exists it is one of the forms in the eigenfunctions, assuming that the boundary conditions near $r = 0$ of the wedge are homogeneous (Ting, 1996).

A logarithmic stress singularity may also occur when the boundary conditions near $r = 0$ of the wedge are not homogeneous.

Although the presence of the logarithmic singularity may be sufficient to cause delamination at the free edge of composite, the role of the possible $r^{\lambda-1}$ singularity should not be ignored. The $r^{\lambda-1}$ singularity is much stronger than the logarithmic singularity and, if present, can be primarily responsible for the onset of delamination (Stolarski and Chiang, 1989). The results obtained in this approach are based on the consideration of the $r^{\lambda-1}$ type stress singularity only. The existence of logarithmic solutions should also be checked.

2. Governing equations for an anisotropic wedge in the generalized plane strain state

2.1. General formulation

A single-material anisotropic wedge of uniform cross-section is shown in Fig. 1. The wedge angle is 2α $(0 < \alpha < \pi)$. The global coordinate Oxyz is defined such that x–y plane represents the geometrically symmetric surface. The body possesses rectilinear anisotropy and the applied tractions do not vary along the longitudinal z-direction. The dimension of the body in the z-direction is large enough to warrant the assumption that the stresses and displacements are independent of the z-coordinate. Since the material is anisotropic, the x–y plane is not a plane of symmetry. Therefore, despite the fact that the problem is two dimensional, the x–y plane will not remain plane after deformation, and the stress states will be three-dimensional. This type of deformation is referred to as "generalized plane strain" or "generalized plane deformation". For this situation, Lekhnitskii has developed a formulation in terms of complex variables $\phi_1(z_1)$, $\phi_2(z_2)$ and $\phi_3(z_3)$ to express the stress components in the form

$$\begin{aligned}
\sigma_x &= 2\mathrm{Re}[\mu_1^2\phi_1'(z_1) + \mu_2^2\phi_2'(z_2) + \mu_3^2\Lambda_3\phi_3'(z_3)]\\
\sigma_y &= 2\mathrm{Re}[\phi_1'(z_1) + \phi_2'(z_2) + \Lambda_3\phi_3'(z_3)]\\
\tau_{xy} &= -2\mathrm{Re}[\mu_1\phi_1'(z_1) + \mu_2\phi_2'(z_2) + \mu_3\Lambda_3\phi_3'(z_3)]\\
\tau_{xz} &= 2\mathrm{Re}[\mu_1\Lambda_1\phi_1'(z_1) + \mu_2\Lambda_2\phi_2'(z_2) + \mu_3\phi_3'(z_3)]\\
\tau_{yz} &= -2\mathrm{Re}[\Lambda_1\phi_1'(z_1) + \Lambda_2\phi_2'(z_2) + \phi_3'(z_3)]
\end{aligned} \tag{1}$$

where

$$z_i = x + \mu_i y \quad i = 1, 2, 3 \tag{2}$$

and constants μ_i are the roots of the following characteristic equation:

$$l_4(\mu)l_2(\mu) - l_3^2(\mu) = 0 \tag{3}$$

with

$$\begin{aligned}
l_2(\mu) &= \beta_{55}\mu^2 - 2\beta_{45}\mu + \beta_{44}\\
l_3(\mu) &= \beta_{15}\mu^3 - (\beta_{14} + \beta_{56})\mu^2 + (\beta_{25} + \beta_{46})\mu - \beta_{24}\\
l_4(\mu) &= \beta_{11}\mu^4 - 2\beta_{16}\mu^3 + (2\beta_{12} + \beta_{66})\mu^2 - 2\beta_{26}\mu + \beta_{22}.
\end{aligned} \tag{4}$$

In the above, β_{ij} are the terms in the reduced elastic compliance matrix.

For an anisotropic material, the stress–strain relations can be written as:

$$\begin{bmatrix} \varepsilon_x \\ \varepsilon_y \\ \varepsilon_z \\ \gamma_{yz} \\ \gamma_{xz} \\ \gamma_{xy} \end{bmatrix} = \begin{bmatrix} a_{11} & a_{12} & a_{13} & a_{14} & a_{15} & a_{16} \\ a_{12} & a_{22} & a_{23} & a_{24} & a_{25} & a_{26} \\ a_{13} & a_{23} & a_{33} & a_{34} & a_{35} & a_{36} \\ a_{14} & a_{24} & a_{34} & a_{44} & a_{45} & a_{46} \\ a_{15} & a_{25} & a_{35} & a_{45} & a_{55} & a_{56} \\ a_{16} & a_{26} & a_{36} & a_{46} & a_{56} & a_{66} \end{bmatrix} \begin{bmatrix} \sigma_x \\ \sigma_y \\ \sigma_z \\ \tau_{yz} \\ \tau_{xz} \\ \tau_{xy} \end{bmatrix} \tag{5}$$

where a_{ij} $(i,j = 1,\ldots,6)$ are the elastic constants. β_{ij} in Eq. (4) are related to a_{ij} by

$$\beta_{ij} = a_{ij} - \frac{a_{i3}a_{j3}}{a_{33}}, \quad i,j = 1,2,4,5,6. \tag{6}$$

Lekhnitskii (1963) has shown that, for anisotropic materials, Eq. (3) cannot have real roots and that the complex parameters μ_i occur in three pairs of complex conjugate numbers.

In the expressions of Eq. (1), the parameters Λ_1, Λ_2 and Λ_3 are defined as follows:

$$\Lambda_1 = -\frac{l_3(\mu_1)}{l_2(\mu_1)}, \qquad \Lambda_2 = -\frac{l_3(\mu_2)}{l_2(\mu_2)}, \qquad \Lambda_3 = -\frac{l_3(\mu_3)}{l_4(\mu_3)}. \tag{7}$$

Thus, the stress components of anisotropic elasticity problems under the generalized plane strain state are reduced to the determination of three complex potentials $\phi_1(z_1)$, $\phi_2(z_2)$ and $\phi_3(z_3)$ which satisfy the conditions for traction and/or displacements along the boundaries.

2.2. Governing equations for free-edge anisotropic wedges

The cylindrical coordinates (r,θ,z) are used for convenience to express the stress components on boundaries. The transformation is as follows:

$$\begin{aligned} \sigma_\theta &= n^2\sigma_x + m^2\sigma_y - 2mn\tau_{xy} \\ \tau_{\theta r} &= -mn\sigma_x + mn\sigma_y + (m^2 - n^2)\tau_{xy} \\ \tau_{\theta z} &= -n\tau_{xz} + m\tau_{yz} \end{aligned} \tag{8}$$

where $m = \cos\theta$ and $n = \sin\theta$. Substituting Eq. (1) into Eq. (8), the stress components are given as:

$$\sigma_\theta = 2\mathrm{Re}[g_1\phi_1'(z_1) + g_2\phi_2'(z_2) + g_3\Lambda_3\phi_3'(z_3)] \tag{9a}$$

$$\tau_{\theta r} = 2\mathrm{Re}[h_1\phi_1'(z_1) + h_2\phi_2'(z_2) + h_3\Lambda_3\phi_3'(z_3)] \tag{9b}$$

$$\tau_{\theta z} = -2\mathrm{Re}[j_1\Lambda_1\phi_1'(z_1) + j_2\Lambda_2\phi_2'(z_2) + j_3\phi_3'(z_3)] \tag{9c}$$

with

$$\begin{aligned} g_i(\theta) &= n^2\mu_i^2 + m^2 + 2mn\mu_i \\ h_i(\theta) &= -mn\mu_i^2 + mn + (n^2 - m^2)\mu_i \quad i = 1,2,3 \\ j_i(\theta) &= n\mu_i + m. \end{aligned} \tag{10}$$

The boundary surfaces $(\theta = \pm\alpha)$ of the elastic body are stress-free, i.e.

$$\sigma_\theta(\theta = \pm\alpha) = \tau_{\theta r}(\theta = \pm\alpha) = \tau_{\theta z}(\theta = \pm\alpha) = 0. \tag{11}$$

In order to obtain the local solution near the apex of the wedge, the three complex stress potentials $\phi_1(z_1)$, $\phi_2(z_2)$ and $\phi_3(z_3)$ are assumed as follows:

$$\begin{aligned}\phi_1(z_1) &= a_1 z_1^{\lambda} + a_2 \overline{z_1^{\lambda}} \\ \phi_2(z_2) &= b_1 z_2^{\lambda} + b_2 \overline{z_2^{\lambda}} \\ \phi_3(z_3) &= c_1 z_3^{\lambda} + c_2 \overline{z_3^{\lambda}}\end{aligned} \tag{12}$$

where a_1, a_2, b_1, b_2, c_1 and c_2 are complex unknown constants. λ is a complex eigenvalue to be determined.

The variable z_i, defined by Eq. (2), can be written in cylindrical coordinates as:

$$z_i = r(\cos\theta + \mu_i \sin\theta) \equiv r\xi_i(\theta). \tag{13}$$

Substituting Eqs. (12) and (13) into the stress components of Eqs. (9a)–(9c), the boundary conditions (Eq. (11)) yield, for $\theta = \alpha$

$$g_1(\alpha)a_1\xi_1^{\lambda-1}(\alpha) + \overline{g_1(\alpha)a_2\xi_1(\alpha)}^{\lambda-1} + g_2(\alpha)b_1\xi_2^{\lambda-1}(\alpha) + \overline{g_2(\alpha)b_2\xi_2(\alpha)}^{\lambda-1} + g_3(\alpha)\Lambda_3 c_1\xi_3^{\lambda-1}(\alpha) + \overline{g_3(\alpha)\Lambda_3 c_2\xi_3(\alpha)}^{\lambda-1} = 0 \tag{14a}$$

$$h_1(\alpha)a_1\xi_1^{\lambda-1}(\alpha) + \overline{h_1(\alpha)a_2\xi_1(\alpha)}^{\lambda-1} + h_2(\alpha)b_1\xi_2^{\lambda-1}(\alpha) + \overline{h_2(\alpha)b_2\xi_2(\alpha)}^{\lambda-1} + h_3(\alpha)\Lambda_3 c_1\xi_3^{\lambda-1}(\alpha) + \overline{h_3(\alpha)\Lambda_3 c_2\xi_3(\alpha)}^{\lambda-1} = 0 \tag{14b}$$

$$j_1(\alpha)\Lambda_1 a_1\xi_1^{\lambda-1}(\alpha) + \overline{j_1(\alpha)\Lambda_1 a_2\xi_1(\alpha)}^{\lambda-1} + j_2(\alpha)\Lambda_2 b_1\xi_2^{\lambda-1}(\alpha) + \overline{j_2(\alpha)\Lambda_2 b_2\xi_2(\alpha)}^{\lambda-1} + j_3(\alpha)c_1\xi_3^{\lambda-1}(\alpha) + \overline{j_3(\alpha)c_2\xi_3(\alpha)}^{\lambda-1} = 0 \tag{14c}$$

and, for $\theta = -\alpha$

$$g_1(-\alpha)a_1\xi_1^{\lambda-1}(-\alpha) + \overline{g_1(-\alpha)a_2\xi_1(-\alpha)}^{\lambda-1} + g_2(-\alpha)b_1\xi_2^{\lambda-1}(-\alpha) + \overline{g_2(-\alpha)b_2\xi_2(-\alpha)}^{\lambda-1} + g_3(-\alpha)\Lambda_3 c_1\xi_3^{\lambda-1}(-\alpha) + \overline{g_3(-\alpha)\Lambda_3 c_2\xi_3(-\alpha)}^{\lambda-1} = 0 \tag{14d}$$

$$h_1(-\alpha)a_1\xi_1^{\lambda-1}(-\alpha) + \overline{h_1(-\alpha)a_2\xi_1(-\alpha)}^{\lambda-1} + h_2(-\alpha)b_1\xi_2^{\lambda-1}(-\alpha) + \overline{h_2(-\alpha)b_2\xi_2(-\alpha)}^{\lambda-1} + h_3(-\alpha)\Lambda_3 c_1\xi_3^{\lambda-1}(-\alpha) + \overline{h_3(-\alpha)\Lambda_3 c_2\xi_3(-\alpha)}^{\lambda-1} = 0 \tag{14e}$$

$$j_1(-\alpha)\Lambda_1 a_1\xi_1^{\lambda-1}(-\alpha) + \overline{j_1(-\alpha)\Lambda_1 a_2\xi_1(-\alpha)}^{\lambda-1} + j_2(-\alpha)\Lambda_2 b_1\xi_2^{\lambda-1}(-\alpha) + \overline{j_2(-\alpha)\Lambda_2 b_2\xi_2(-\alpha)}^{\lambda-1} + j_3(-\alpha)c_1\xi_3^{\lambda-1}(-\alpha) + \overline{j_3(-\alpha)c_2\xi_3(-\alpha)}^{\lambda-1} = 0. \tag{14f}$$

Eqs. (14a)–(14f) are six linear homogeneous equations with unknowns a_1, $\overline{a_2}$, b_1, $\overline{b_2}$, c_1 and $\overline{c_2}$. They can be rewritten in the following matrix form

$$\mathbf{M}(\lambda)\mathbf{v} = \mathbf{0} \tag{15}$$

where the vector $\mathbf{v}$ is

$$\mathbf{v} = \{a_1, \overline{a_2}, b_1, \overline{b_2}, c_1, \overline{c_2}\}^{\mathrm{T}}. \tag{16}$$

For non-trivial solutions of vector $\mathbf{v}$, the determinant of the matrix $\mathbf{M}(\lambda)$ must vanish, i.e.

$$\det\{\mathbf{M}(\lambda)\} = 0. \tag{17}$$

An explicit expression for the determinant as a function of the eigenvalues λ is too complicated to be shown here. Of all the infinite numbers of λ, only a small number of eigenvalues are of interest. Eigenvalues with $0 < \mathrm{Re}[\lambda] < 1$ result in stress singularities, i.e. infinitely large stresses at the apex of the wedge.

2.3. Decoupled inplane and antiplane stress field

When the fibers lie in the x–y plane, the material constants a_{14}, a_{15}, a_{24}, a_{25}, a_{34}, a_{35}, a_{46} and a_{56} in Eq. (5) vanish. Consequently, the constants β_{14}, β_{15}, β_{24}, β_{25}, β_{46} and β_{56} in Eq. (6) become zero. From Eq. (4), $l_3(\mu) = 0$. Substituting into Eq. (3), it gives

$$l_2(\mu) = 0 \tag{18}$$

$$l_4(\mu) = 0. \tag{19}$$

The roots of Eq. (19), defined as μ_1 and μ_2, correspond to the inplane field. Meanwhile, the roots of Eq. (18), defined as μ_3, correspond to the antiplane field. From Eq. (7), the parameters Λ_1, Λ_2 and Λ_3 are zero. Therefore, the matrix $\mathbf{M}(\lambda)$ is reduced to the form:

$$\begin{vmatrix} g_1(\alpha)\xi_1^{\lambda-1}(\alpha) & \overline{g_1(\alpha)\xi_1(\alpha)}^{\lambda-1} & g_2(\alpha)\xi_2^{\lambda-1}(\alpha) & \overline{g_2(\alpha)\xi_2(\alpha)}^{\lambda-1} & 0 & 0 \\ h_1(\alpha)\xi_1^{\lambda-1}(\alpha) & \overline{h_1(\alpha)\xi_1(\alpha)}^{\lambda-1} & h_2(\alpha)\xi_2^{\lambda-1}(\alpha) & \overline{h_2(\alpha)\xi_2(\alpha)}^{\lambda-1} & 0 & 0 \\ 0 & 0 & 0 & 0 & j_3(\alpha)\xi_3^{\lambda-1}(\alpha) & \overline{j_3(\alpha)\xi_3(\alpha)}^{\lambda-1} \\ g_1(-\alpha)\xi_1^{\lambda-1}(-\alpha) & \overline{g_1(-\alpha)\xi_1(-\alpha)}^{\lambda-1} & g_2(-\alpha)\xi_2^{\lambda-1}(-\alpha) & \overline{g_2(-\alpha)\xi_2(-\alpha)}^{\lambda-1} & 0 & 0 \\ h_1(-\alpha)\xi_1^{\lambda-1}(-\alpha) & \overline{h_1(-\alpha)\xi_1(-\alpha)}^{\lambda-1} & h_2(-\alpha)\xi_2^{\lambda-1}(-\alpha) & \overline{h_2(-\alpha)\xi_2(-\alpha)}^{\lambda-1} & 0 & 0 \\ 0 & 0 & 0 & 0 & j_3(-\alpha)\xi_3^{\lambda-1}(-\alpha) & \overline{j_3(-\alpha)\xi_3(-\alpha)}^{\lambda-1} \end{vmatrix} = 0 \tag{20}$$

After rearranging Eq. (20) can be decoupled into the following two equations:

$$\begin{vmatrix} g_1(\alpha)\xi_1^{\lambda-1}(\alpha) & \overline{g_1(\alpha)\xi_1(\alpha)}^{\lambda-1} & g_2(\alpha)\xi_2^{\lambda-1}(\alpha) & \overline{g_2(\alpha)\xi_2(\alpha)}^{\lambda-1} \\ h_1(\alpha)\xi_1^{\lambda-1}(\alpha) & \overline{h_1(\alpha)\xi_1(\alpha)}^{\lambda-1} & h_2(\alpha)\xi_2^{\lambda-1}(\alpha) & \overline{h_2(\alpha)\xi_2(\alpha)}^{\lambda-1} \\ g_1(-\alpha)\xi_1^{\lambda-1}(-\alpha) & \overline{g_1(-\alpha)\xi_1(-\alpha)}^{\lambda-1} & g_2(-\alpha)\xi_2^{\lambda-1}(-\alpha) & \overline{g_2(-\alpha)\xi_2(-\alpha)}^{\lambda-1} \\ h_1(-\alpha)\xi_1^{\lambda-1}(-\alpha) & \overline{h_1(-\alpha)\xi_1(-\alpha)}^{\lambda-1} & h_2(-\alpha)\xi_2^{\lambda-1}(-\alpha) & \overline{h_2(-\alpha)\xi_2(-\alpha)}^{\lambda-1} \end{vmatrix} = 0 \tag{21}$$

$$\begin{vmatrix} j_3(\alpha)\xi_3^{\lambda-1}(\alpha) & \overline{j_3(\alpha)\xi_3(\alpha)}^{\lambda-1} \\ j_3(-\alpha)\xi_3^{\lambda-1}(-\alpha) & \overline{j_3(-\alpha)\xi_3(-\alpha)}^{\lambda-1} \end{vmatrix} = 0. \tag{22}$$

It is noted that the parameters and singularity orders in Eqs. (21) and (22) are only associated with the inplane and antiplane fields, respectively.

3. The definition of a quarter circular region

This paper is concerned with the orders of stress singularity for fiber reinforced composite materials with an arbitrary fiber orientation. Consider a fiber OD of the composite material in space (Fig. 2). The components of unit vector **f** directed along the fiber are all positive. Assume that the projection of **f** on the x–y plane is **p**. The angle between **f** and **p** is ξ, while the angle between **p** and the positive x-axis is η. Thus, the coordinate pair (ξ, η) defines the fiber direction. Due to symmetry, only fiber vectors in the first quadrant are considered for one-material wedge problems. The others can be ignored.

One-quarter circular region is proposed as shown in Fig. 3. All possible values of fiber direction (ξ, η) can be located in this region. The definition of (ξ, η) is similar to the radial and tangential directions in polar coordinate system. The units of ξ and η are degrees, and their values are in the range $0° \leqslant \xi, \eta \leqslant 90°$. It is clear that any point in the region corresponds to the projection of point D on the x–y plane. Three lines bound the region. The curved line O_xO_y ($\xi = 0°$) represents that the fibers that lie in the x–y plane and

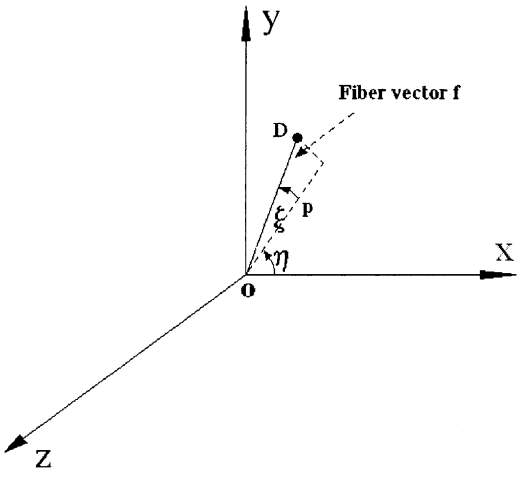

Fig. 2. The definition of the fiber orientation in space.

make an angle η with the positive x-axis. Lines O_xO_z ($\eta = 0°$) and O_yO_z ($\eta = 90°$) are the cases in which the fibers lie in the x–z and y–z planes, respectively. The points O_x, O_y and O_z correspond to the cases that the fibers are parallel to the x-axis, y-axis and z-axis, respectively.

All curves plotted in the region are the contours of the stress singularity order $\lambda - 1$. For example, the contour in Fig. 3(a) denotes the variation of largest root $|\lambda_1 - 1|$ ($0 < \mathrm{Re}[\lambda] < 1$) as $2\alpha = 270°$. This case will be discussed in the next section.

4. Results and discussion

4.1. An anisotropic wedge with arbitrary fiber orientation

A typical graphite–epoxy unidirectional composite material is considered in this study. The engineering constants of this fiber-reinforced composite adopted are assumed as (Wang and Crossman, 1977):

$$\begin{aligned} &E_{\mathrm{L}} = 137.90\ \mathrm{GPa}, \quad E_{\mathrm{T}} = E_{\mathrm{Z}} = 14.48\ \mathrm{GPa} \\ &G_{\mathrm{LT}} = G_{\mathrm{LZ}} = G_{\mathrm{TZ}} = 5.86\ \mathrm{GPa} \\ &v_{\mathrm{LT}} = v_{\mathrm{LZ}} = v_{\mathrm{TZ}} = 0.21 \end{aligned} \tag{23}$$

where E, G and v are the Young's modulus, shear modulus and Possion's ratio, respectively. The subscript L refers to the fiber direction, and T lies in the x–y plane and is normal to the L-axis. Z is normal to the L–T plane according to the right-hand rule. The direction of the L-axis is denoted as (ξ, η) defined in Section 3. The material constants a_{ij} ($i, j = 1, \ldots, 6$) in Eq. (5) correspond to the xyz coordinates and can be obtained by coordinate transformation. Thus, the composite material which can be considered as orthotropic in the (L, T, Z) coordinate system is fully anisotropic in the (x, y, z) coordinate system.

For wedge angle $2\alpha = 270°$, there are three eigenvalues in solving the eigen-equation $|\mathbf{M}(\lambda)| = 0$. Fig. 3(a)–(c) show the contours of singularity orders $\lambda_i - 1$ ($i = 1, 2, 3$).

As discussed in Section 2.3, the inplane and antiplane problems of any anisotropic wedge with fibers which lie in the x–y plane ($\xi = 0°$) are decoupled. In Fig. 3, all singularity orders $\lambda - 1$ on curve O_xO_y ($\xi = 0°$) are related to results of Bogy (1972) and Ma (1989). Table 1 lists the values of $(\lambda - 1)$ computed

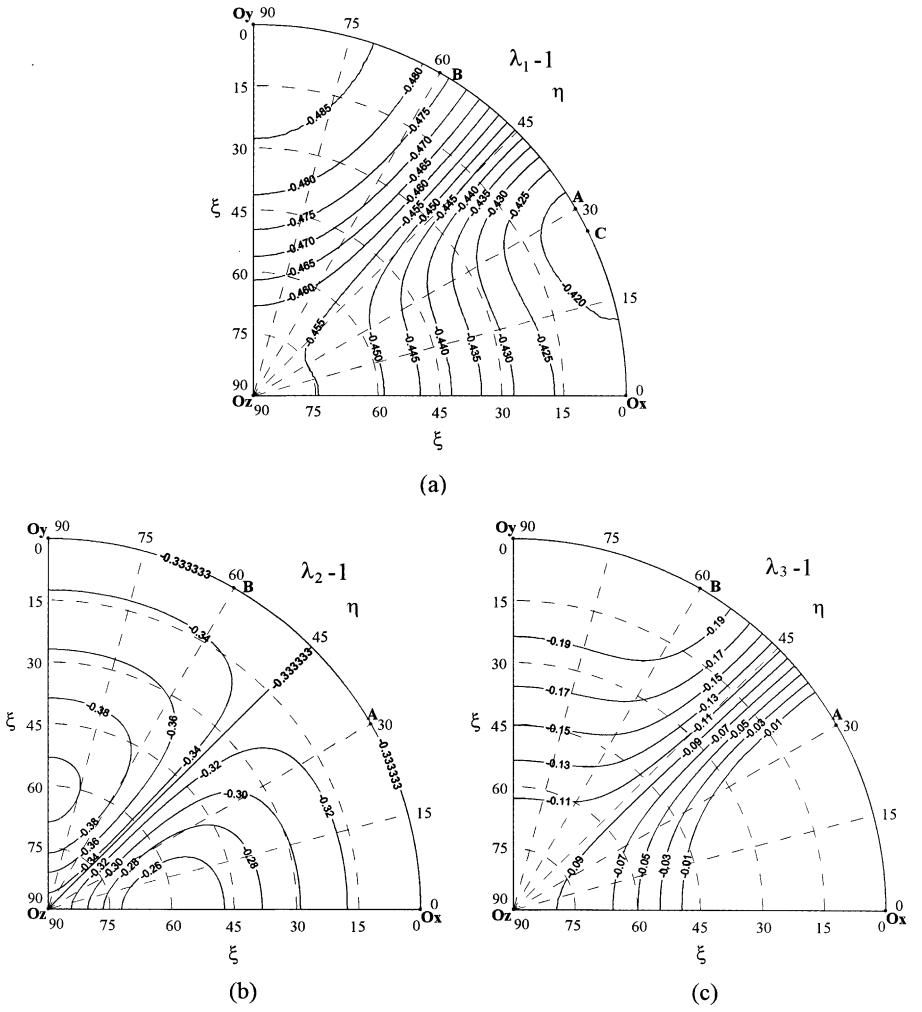

Fig. 3. Contours of stress singularity order ($2\alpha = 270°$) (a) the first root $\lambda_1 - 1$; (b) the second root $\lambda_2 - 1$ and (c) the third root $\lambda_3 - 1$.

Table 1
The stress singularity orders ($\lambda - 1$) for an orthotropic wedge ($2\alpha = 270°$)

	$\eta = 0°$	$\eta = 30°$	$\eta = 60°$	$\eta = 90°$
Present paper				
	−0.4213367308	−0.4182463223	−0.4769643917	−0.4882001112
	−0.333333	−0.333333	−0.333333	−0.333333
			−0.204754671	−0.2057103419
Bogy (1972)				
	−0.4213367308	−0.4182463223	−0.4769643917	−0.4882001112
			−0.204754671	−0.2057103419
Ma (1989)				
	−0.333333	−0.333333	−0.333333	−0.333333

from present paper, Bogy and Ma when $2\alpha = 270°$. In the present approach, the singularity orders corresponding to the inplane and antiplane problems can be obtained simultaneously (Fig. 3(a)–(c)). It is observed that:

(a) As $(\xi, \eta) = (0°, 0°)$, point O_x of Fig. 3(a) gives the inplane singularity order $\lambda_1 - 1 = -0.4213367308$ and point O_x of Fig. 3(b) gives the antiplane singularity order $\lambda_2 - 1 = -0.33333$. The third order $\lambda_3 - 1$ is zero (point O_x of Fig. 3(c)).

(b) As $(\xi, \eta) = (0°, 90°)$, point O_y of Fig. 3(a) gives the inplane singularity order $\lambda_1 - 1 = -0.4882001112$ and point O_y of Fig. 3(b) gives the antiplane singularity order $\lambda_2 - 1 = -0.33333$. The third order $\lambda_3 - 1 = -0.2057103419$ for the inplane case (point O_y of Fig. 3(c)).

Same discussions can be made on points A ($\eta = 30°$) and B ($\eta = 60°$) in Fig. 3. From Table 1, good agreements with published results have been verified. It concludes that the results of Bogy and Ma are only the special cases of present approach.

Minimum of $|\lambda_1 - 1|$ in Fig. 3 is generally desired to diminish the stress concentration near the tip. From Fig. 3(a), the smallest $|\lambda_1 - 1|$ is 0.4175018 for $\xi = 0°$ and $\eta = 25.6°$, i.e. at point C.

4.2. The singularity orders of a crack in an orthotropic material

Now consider the case with $(\xi, \eta) = (0°, 0°)$ and $2\alpha = 360°$, i.e. a crack exists in an orthotropic composite. The singularity orders of the inplane and antiplane problems are all -0.5. The solution of formulation in this approach breaks down as $2\alpha = 360°$. To make it possible to analyze a crack problem, the wedge angle has to be modified slightly, e.g. $2\alpha = 359.9998°$. The computed orders of stress singularity are -0.4999995 of triple roots. Two roots correspond to the inplane problem and the other is for the antiplane problem. Fig. 4 shows the contours of the first root $\lambda_1 - 1$. They are very close to -0.5. This example further validates the formulation.

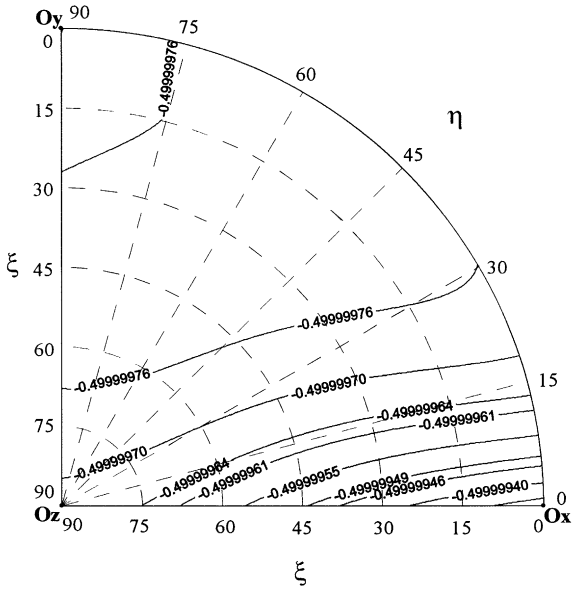

Fig. 4. Contours of the first singularity order $\lambda_1 - 1$ for $2\alpha = 359.9998°$.

4.3. A single-material wedge with isotropic material

For an isotropic material, the complex parameters μ_i defined in Eq. (3) are pair equal and Lekhnitskii's formulation is not valid. In order to make the analysis for an isotropic body possible, the following method of perturbing the isotropic material properties E and v has been proposed (Lin and Hartmann, 1989).

$$E_L = E, \quad E_T = (1+\varepsilon)E, \quad E_Z = (1-\varepsilon)E; \qquad G_{TL} = G_{TZ} = G_{LZ} = E/[2(1+v)];$$
$$v_{TL} = v_{TZ} = v_{LZ} = v \tag{24}$$

where ε is a small constant, say 10^{-5} or 10^{-7}. After this modification, the roots of Eq. (3) are distinct and the present formulation still works.

Williams (1952) and Ma (1989) computed the stress singularity orders for an isotropic wedge under the inplane and antiplane loading conditions, respectively. Fig. 5 shows the contours of singularity order $\lambda_1 - 1$. The values of contours are close to -0.4555163 obtained by Williams. Table 2 shows the numerical results as $2\alpha = 200°$ and $270°$. Accurate results are guaranteed if ε is small enough.

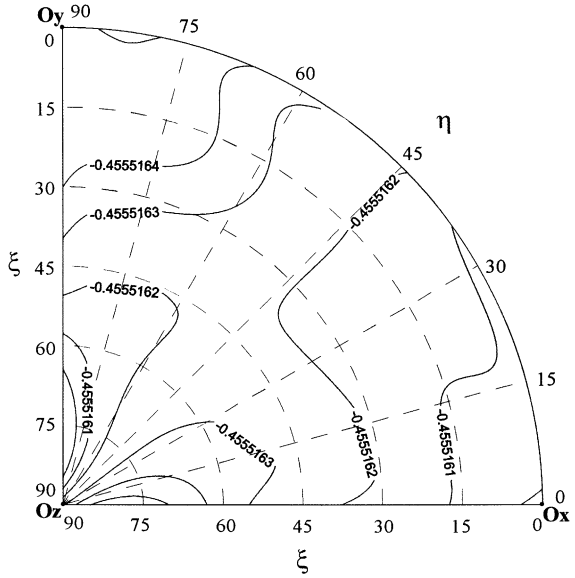

Fig. 5. Contours of singularity order $\lambda_1 - 1$ for isotropic material ($2\alpha = 270°$).

Table 2
The stress singularity orders for an isotropic wedge

Wedge angle	Inplane	Antiplane	Present paper	
	Williams (1952)	Ma (1989)	$\varepsilon = 10^{-5}$	$\varepsilon = 10^{-7}$
$2\alpha = 200°$	−0.1813041	−0.1	−0.1813038	−0.1813041
			−0.09999978	−0.1
$2\alpha = 270°$	−0.4555163		−0.4555161	−0.4555163
		−0.3333333	−0.333333	−0.3333333
	−0.09147081		−0.09146986	−0.09147081

4.4. The fiber orientation (ξ^*, η^*) corresponding to the minimum stress singularity order at different wedge angle

If wedge shapes exist in composite structure, it is necessary to reduce the strength of stress singularity, i.e. $(\lambda - 1)$. The order depends on the wedge angle 2α, the fiber orientation (ξ, η), and the material constants. This section studies all of these three factors. With this, the fiber orientation corresponding to the minimum stress singularity order, which is denoted as (ξ^*, η^*), can be found to reduce the stress concentration near the tip.

4.4.1. The factors of wedge angle 2α and fiber orientation (ξ^*, η^*)

Since there is no stress singularity for $2\alpha \leqslant 180°$, the discussion on wedge angle is in the range $180° < 2\alpha < 360°$. Figs. 6–9 display the contours of the first singularity order $\lambda_1 - 1$ at different angles. For all cases, the highest values of $|\lambda_1 - 1|$, i.e. the strongest stress singularities, occur at point O_y. It indicates that the fiber orientation should not coincide with the y-axis. Moreover, the minimum of $|\lambda_1 - 1|$ are all on the arc O_xO_y ($\xi^* = 0°$). Table 3 lists the minimum of $|\lambda_1 - 1|$ and the associated fiber angles η^* at different

Table 3
The minimum of $|\lambda_1 - 1|$ (inplane), $|\lambda_2 - 1|$ (antiplane) and the associated fiber orientations (ξ^*, η^*) at different wedge angles

2α	Inplane			Antiplane		
	ξ^*	η^*	$\lambda_1 - 1$	ξ^*	η^*	$\lambda_2 - 1$
200°	0°	44.7°	−0.1283047	0°	$0° \leqslant \eta \leqslant 90°$	−0.1
250°	0°	35.2°	−0.3592504	0°	$0° \leqslant \eta \leqslant 90°$	−0.28
270°	0°	25.6°	−0.4175018	0°	$0° \leqslant \eta \leqslant 90°$	−0.3
300°	0°	0°	−0.4659950	0°	$0° \leqslant \eta \leqslant 90°$	−0.4
350°	0°	0°	−0.4995973	0°	$0° \leqslant \eta \leqslant 90°$	−0.4857

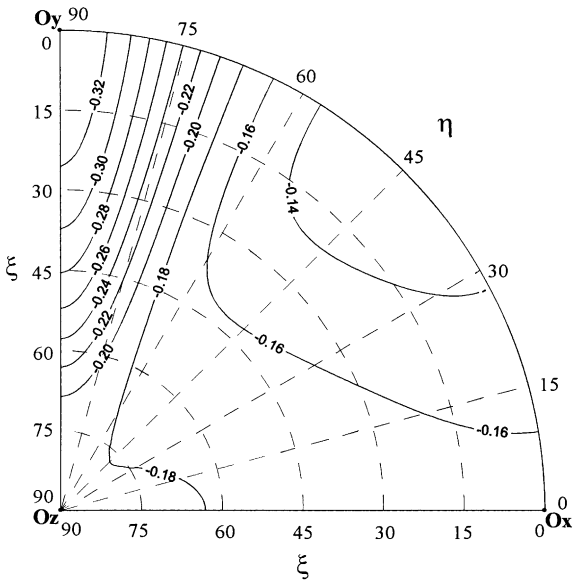

Fig. 6. Contours of the first singularity order $\lambda_1 - 1$ for $2\alpha = 200°$.

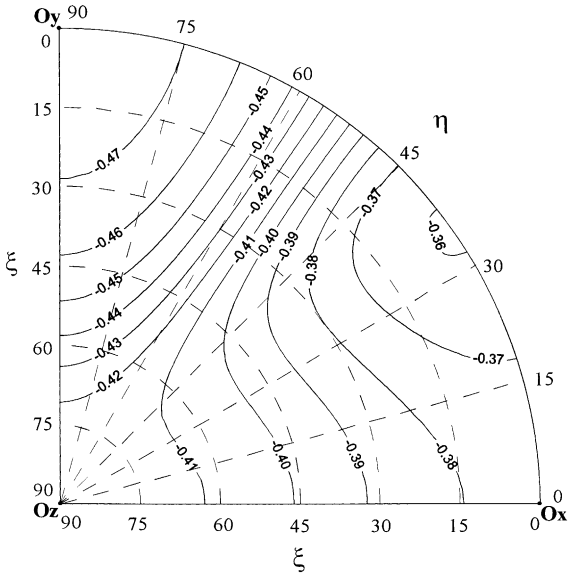

Fig. 7. Contours of the first singularity order $\lambda_1 - 1$ for $2\alpha = 250°$.

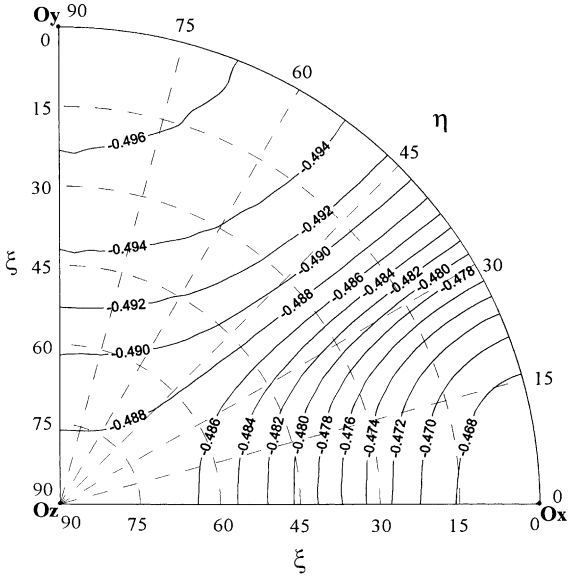

Fig. 8. Contours of the first singularity order $\lambda_1 - 1$ for $2\alpha = 300°$.

wedge angles. The second roots $\lambda_2 - 1$ on arc O_xO_y ($\xi = 0°$, $0° < \eta < 90°$), corresponding to the antiplane problem, are also shown in the table. Consider the case $2\alpha = 270°$. For coupled or decoupled stress field, the

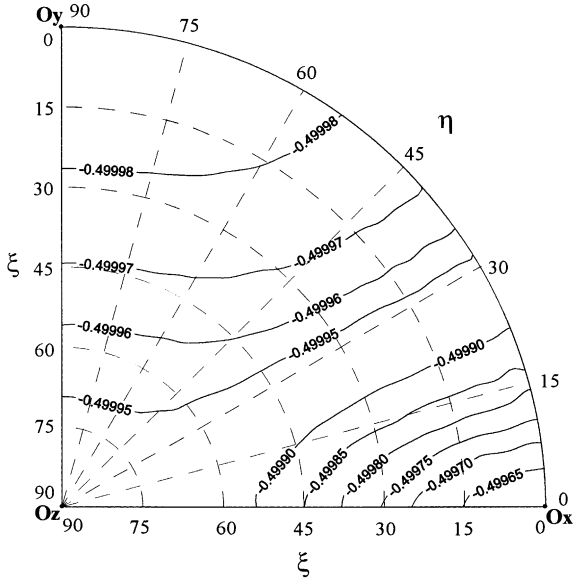

Fig. 9. Contours of the first singularity order $\lambda_1 - 1$ for $2\alpha = 350°$.

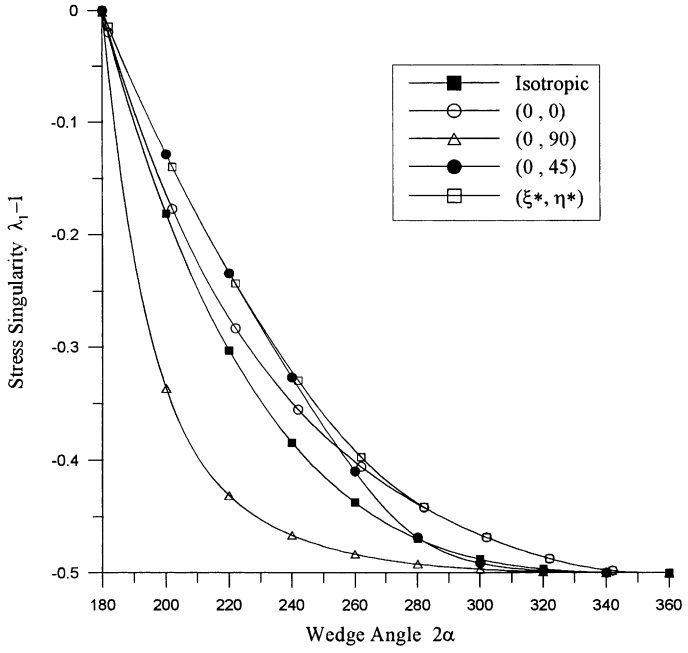

Fig. 10. The variations of the first singularity order $\lambda_1 - 1$ with wedge angle. The minimum singularity order associates with the particular fiber orientation (ξ^*, η^*).

particular fiber orientation (ξ^*, η^*) corresponding to the minimum stress singularity order is $\xi^* = 0°$ and $\eta^* = 25.6°$.

When $\xi = 0°$ and $\eta = 0°, 45°, 90°$, Fig. 10 plots the variations of dominant stress singularity order $\lambda_1 - 1$ with wedge angle 2α at 2° increment. The singularity orders for isotropic wedges are included in the figure. Moreover, the values of smallest $|\lambda_1 - 1|$, depend on η^*, are also plotted for comparison.

4.4.2. The effects of material constants

The influence of material properties on the stress singularity is investigated in this section. Two factors, Young's modulus E_L and shear modulus G_{TZ}, are considered separately.

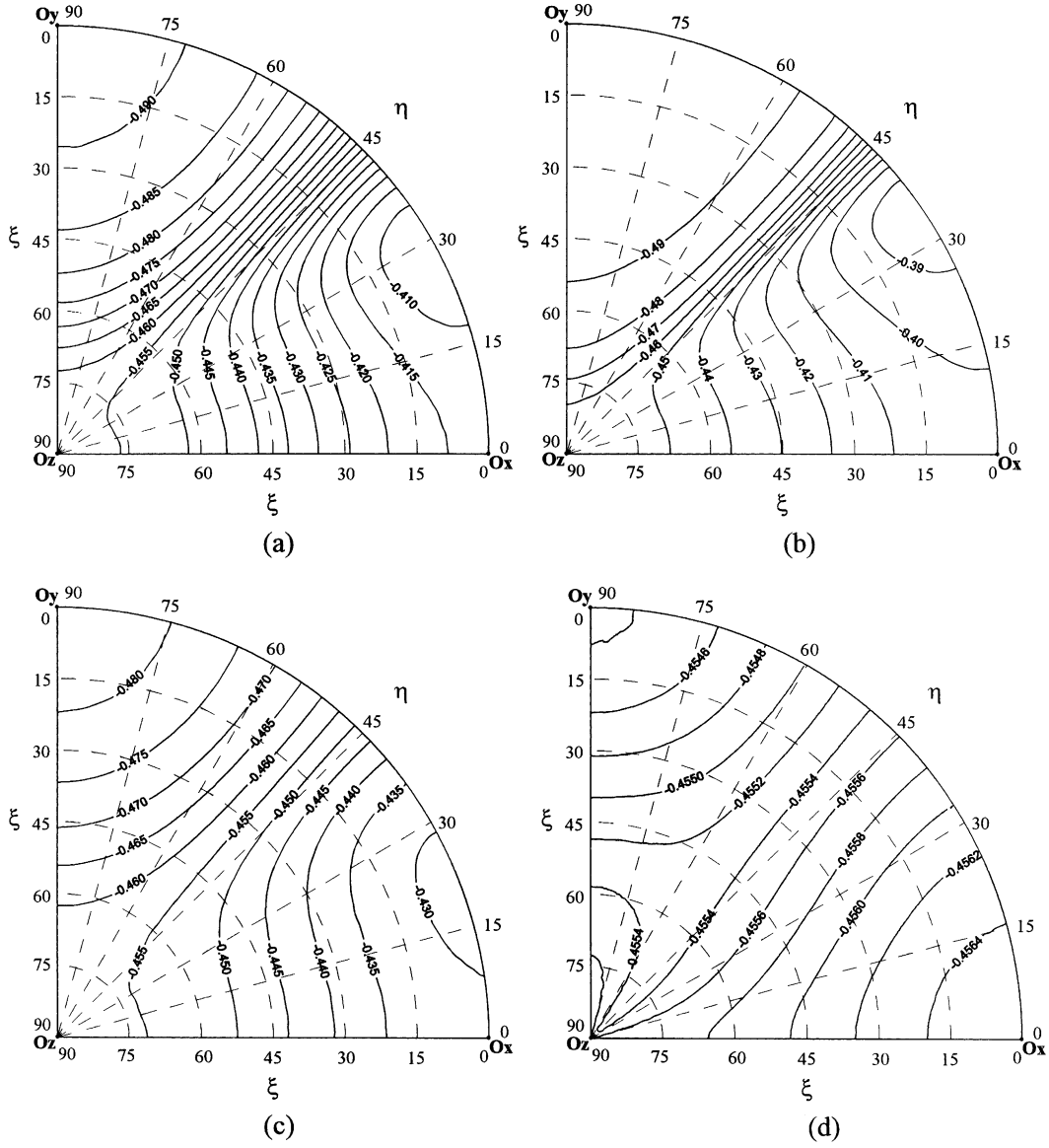

Fig. 11. Contours of the first singularity order $\lambda_1 - 1$ with various E_L for $2\alpha = 270°$ (a) 2 E_L; (b) 10 E_L; (c) 0.5 E_L; (d) 0.1 E_L.

(1) *Young's modulus* E_L. The material constant E_L used in Fig. 3 is 137.9 GPa. Fig. 11 display the contours of stress singularity orders $\lambda_1 - 1$ at various E_L where $2\alpha = 270°$. Comparing with Fig. 3(a), it is shown that the singularity orders decrease in the region $(0° < \xi < 90°,\ 0° < \eta < 45°)$ and increase in the region $(0° < \xi < 90°,\ 45° < \eta < 90°)$ when E_L is increased. It indicates that the minimum singularity orders corresponding to the fiber orientation (ξ^*, η^*) become smaller if the fibers are made stiffer. If the fibers lie along the x-axis $(\xi = 0°, \eta = 0°)$, Fig. 12 shows the variations of the order $\lambda_1 - 1$ with wedge angle when E_L is changed. For the purpose of reducing the stress singularities, the usage of composite materials with stiffer fiber in structural design offers better results if the fiber orientation is properly selected. It is worth noting that values $\lambda_2 - 1$ on O_xO_y do not depend on E_L.

(2) *Shear modulus* G_{TZ}. It has been discussed in previous section that curve O_xO_y in contour lines of the second root $\lambda_2 - 1$ denotes the decoupled antiplane problems. Their magnitudes strongly depend on the shear modulus G_{TZ}. When $2\alpha = 270°$, Fig. 13 displays the contours $\lambda_2 - 1$ when G_{TZ} is reduced to half. Comparing with Fig. 3(b), $\lambda_2 - 1$ on curve O_xO_y have been changed from -0.33333 to variable values, depending on η. For example, $\lambda_2 - 1$ is -0.3076258 at $\eta = 30°$. Again, it is shown that the singularity orders decrease in the region $(0° < \xi < 90°,\ 0° < \eta < 45°)$ and increase in the region $(0° < \xi < 90°,\ 45° < \eta < 90°)$ when G_{TZ} is decreased. If the fibers lie along the x-axis $(\xi = 0°,\ \eta = 0°)$, Fig. 14 shows the variations of the orders $\lambda_2 - 1$ with wedge angle when G_{TZ} is changed. The usage of composite materials with lower G_{TZ} offers better results to reduce stress singularities if the fiber orientation is selected in $0° < \eta < 45°$. Fig. 15 displays the contours of orders $\lambda_1 - 1$ for $0.5G_{TZ}$. Comparing with Fig. 3(a), it shows that values $\lambda_1 - 1$ on curve O_xO_y do not change when G_{TZ} is altered. Fig. 16 displays the minimum of $|\lambda_1 - 1|$ and the associated fiber orientation η^* at different wedge angles.

5. Conclusions

A general solution for determining the stress singularity order in an anisotropic wedge has been presented. Based on the Lekhnitskii's complex function method, the characteristic equation is formulated. The

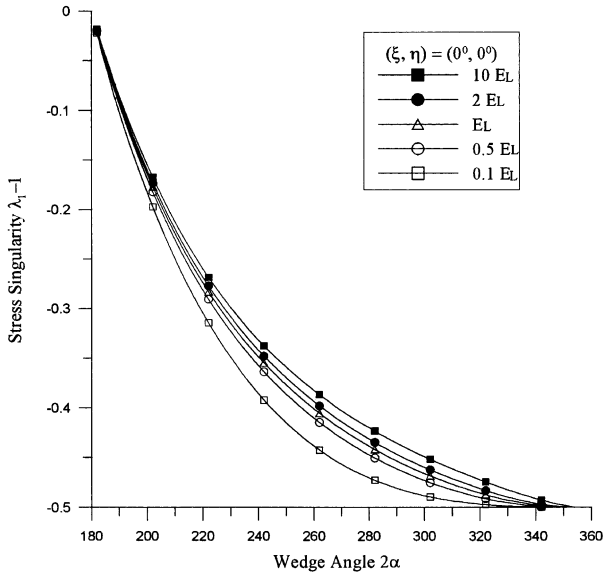

Fig. 12. Comparison of the first singularity orders $\lambda_1 - 1$ at different E_L when $\xi = 0°$ and $\eta = 0°$.

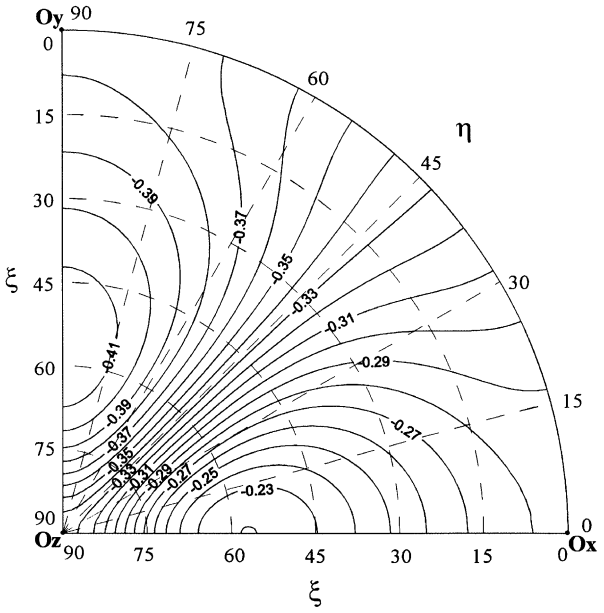

Fig. 13. Contours of the second singularity order $\lambda_2 - 1$ for $0.5G_{TZ}$ at $2\alpha = 270°$.

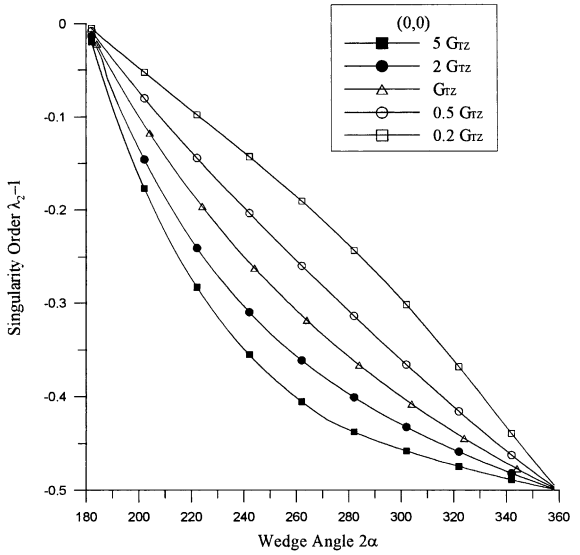

Fig. 14. Comparison of the second singularity orders $\lambda_2 - 1$ at different G_{TZ} when $\xi = 0°$ and $\eta = 0°$.

contours of stress singularity order for arbitrary fiber orientation are plotted in a one-quarter circular region. From this approach, the fiber orientation (ξ^*, η^*) can be determined to reduce the stress singularity at the wedge corner. Moreover, the numerical results for some simple cases agree well with the open literature.

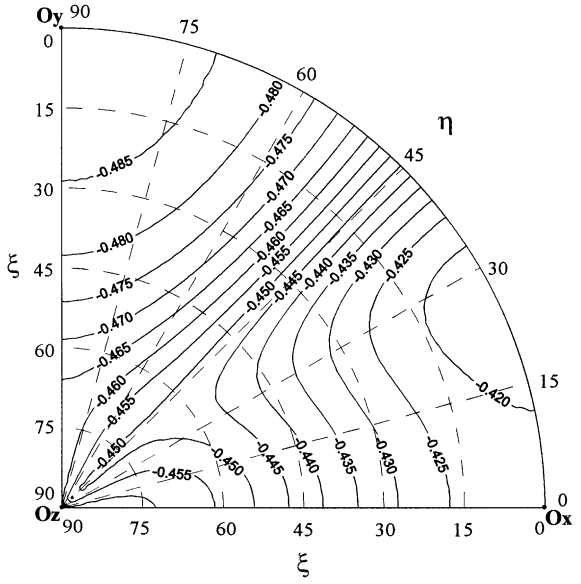

Fig. 15. Contours of the first singularity order $\lambda_1 - 1$ for $0.5G_{TZ}$ and $2\alpha = 270°$.

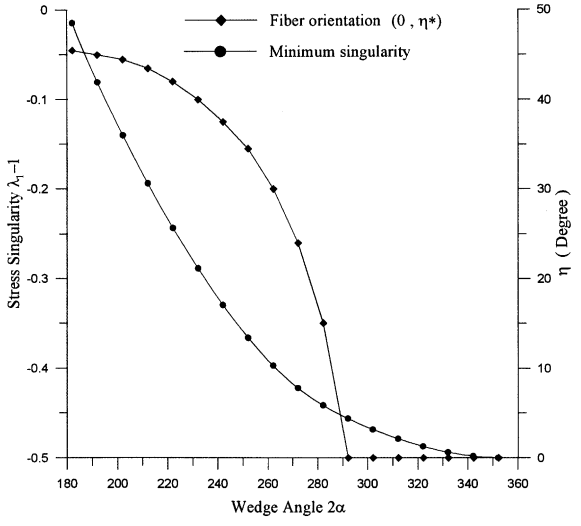

Fig. 16. The minimum values of $|\lambda_1 - 1|$ and the associated fiber orientations $(0°, \eta^*)$ at different wedge angles.

Acknowledgements

The authors are grateful to the National Science Council of the ROC for financial support through grant NSC89-2212-E006-119.

References

Bogy, D.B., 1971. Two edge-bonded elastic wedges of different materials and wedge angles under surface tractions. Journal of Applied Mechanics 38, 377–386.

Bogy, D.B., 1972. The plane solution for anisotropic elastic wedges under normal and shear loading. Journal of Applied Mechanics 39, 1103–1109.

Chen, D.H., Nisitani, H., 1992. Singular stress field in two bonded wedges. Transactions of Japan Society of Mechanical Engineers Series A, 58, 457–464.

Chen, D.H., Nisitani, H., 1993. Logarithmic singular stress field in bonded wedges. Transactions of Japan Society of Mechanical Engineers Series A, 59, 2687–2693.

Chen, H.P., 1998. Stress singularities in anisotropic multi-material wedges and junctions. International Journal of Solids and Structures 35, 1057–1073.

Dempsey, J.P., Sinclair, G.B., 1979. On the stress singularities in the plane elasticity of the composite wedge. Journal of Elasticity 9, 373–391.

Delale, F., 1984. Stress singularities in bonded anisotropic materials. International Journal of Solids and Structures 20, 31–40.

Erdogan, F., 1965. Stress distribution in bonded dissimilar materials with cracks. Journal of Applied Mechanics 32, 403–410.

Green, A.E., Zerna, W., 1954. Theoretical Elasticity. Clarendon, Oxford.

Hein, V.L., Erdogan, F., 1971. Stress singularity in a two-material wedge. International Journal of Fracture Mechanics 7, 317–330.

Huang, T.F., Chen, W.H., 1994. On the free-edge stress singularity of general composite laminates under uniform axial strain. International Journal of Solids and Structures 31, 3139–3151.

Koguchi, H., Tadanobu, I., Toshio, Y., 1993. Stress singularity at the apex in three phase bonded structure. Transactions of Japan Society of Mechanical Engineers Series A, 59, 163–170.

Kuo, M.C., Bogy, D.B., 1974a. Plane solutions for the displacement and traction-displacement problems for anisotropic elastic wedges. Journal of Applied Mechanics 41, 197–202.

Kuo, M.C., Bogy, D.B., 1974b. Plane solutions for traction problems on orthotropic unsymmetrical wedges and symmetrically twinned wedges. Journal of Applied Mechanics 41, 203–208.

Lekhnitskii, S.G., 1963. Theory of Elasticity of an Anisotropic Elastic Body. Holden-Day, New York.

Lin, K.Y., Hartmann, H.H., 1989. Numerical analysis of stress singularities at a bonded anisotropic wedge. Engineering Fracture Mechanics 32, 211–224.

Ma, C.C., Hour, B.L., 1989. Analysis of dissimilar anisotropic wedges subjected to antiplane shear deformation. International Journal of Solids and Structures 25, 1295–1309.

Pageau, S.S., Biggers Jr., S.B., 1996. A finite element approach to three-dimensional singular stress states in anisotropic multi-material wedges and junctions. International Journal of Solids and Structures 33, 33–47.

Sih, G.C., Paris, P.C., Irwin, G.R., 1965. On cracks in rectilinearly anisotropic bodies. International Journal of Fracture Mechanics 1, 189–203.

Stolarski, H.K., Chiang, M.Y.M., 1989. On the significance of the logarithmic term in the free edge stress singularity of composite laminates. International Journal of Solids and Structures 25, 75–93.

Stroh, A.N., 1962. Steady state problems in anisotropic elasticity. Journal of Mathematical Physics 41, 77–103.

Theocaris, P.S., 1974. The order of singularity at a multi-wedge corner of a composite plate. International Journal of Engineering Science 12, 107–120.

Ting, T.C.T., Chou, S.C., 1981. Edge singularities in anisotropic composites. International Journal of Solids and Structures 17, 1057–1068.

Ting, T.C.T., Hoang, P.H., 1984. Singularities at the tip of a crack normal to the interface of an anisotropic layered composite. International Journal of Solids and Structures 20, 439–454.

Ting, T.C.T., 1986. Explicit solution and invariance of the singularities at an interface crack in anisotropic composites. International Journal of Solids and Structures 22, 965–983.

Ting, T.C.T., 1996. Anisotropic Elasticity: theory and applications. Oxford University Press, New York.

Tranter, C.J., 1948. The use of the Mellin transform in finding the stress distribution in an infinite wedge. Quarterly Journal of Mechanics and Applied Mathematics 1, 125–130.

Williams, M.L., 1952. Stress singularities resulting from various boundary conditions in angular corners of plates in extension. Journal of Applied Mechanics 19, 526–528.

Wang, A.S.D., Crossman, F.W., 1977. Some new results on edge effect in symmetric composite laminates. Journal of Composite Materials 11, 92–106.

Wang, S.S., Choi, I., 1982. Boundary-layer effects in composite laminates: Part I – Free-edge stress singularities. Journal of Applied Mechanics 49, 541–548.

Zwiers, R.I., Ting, T.C.T., Spiker, R.L., 1982. On the logarithmic singularity of free-edge stress in laminated composites under uniform extension. Journal of Applied Mechanics 49, 561–569.